Twelfth Australasian Fluid Mechanics Conference
The University of Sydney, Australia 1995

PLIF IMAGING OF NITRIC OXIDE IN HIGH ENTHALPY FLOWS

Philip C. Palma, Timothy J. McIntyre*, A.F.P. Houwing
Aerophysics and Laser-based Diagnostics Research Laboratories
Department of Physics, Australian National University
Canberra, Australian Capital Territory
Australia

*Present address: Department of Physics,
University of Queensland
Brisbane, Queensland
Australia

ABSTRACT

Planar laser-induced fluorescence is performed in a free-piston shock tunnel by using a Raman-shifted tunable excimer laser to excite nitric oxide molecules in the flow. Two different flowfields are examined to test the difficulties associated with applying the technique to shock tunnels: the bluff body flow produced by a 25 mm diameter cylinder; and the oblique shock and expansion fan produced by a 35° half angle wedge. For the cylinder, the maximum flow enthalpy was limited to 4.1 MJ/kg due to high flow luminosity which is produced by metallic contaminants in the flow. A reflective filter is used to reduce the influence of flow luminosity making these measurements feasible. Freestream temperature measurements are in excellent agreement with those predicted from numerical flow calculations. Several higher enthalpy shots (14 MJ/kg) were also performed with the wedge and showed an insignificant amount of contaminant emission.

INTRODUCTION

Planar Laser Induced Fluorescence (PLIF) has recently been applied to the study of shock tunnel flows with great success (Palmer et al. 1994, Houwing et al. 1994). Experimental data obtained from these facilities is crucial for the validation of computer codes used in computational fluid dynamics (CFD). The validated CFD codes then provide a means of confidently predicting inflight behaviour and aid in vehicle design and performance evaluation. PLIF overcomes line-of-sight integration problems associated with other optical techniques (interferometry, schlieren etc.) by using a thin sheet of pulsed laser light to excite a transition in a particular chemical species in the flow. This technique allows two dimensional visualisation of rotational and vibrational temperatures, as well as chemical species number densities. It can provide spatially and temporaly resolved cross sections through the flow, thus allowing three dimensional and transient features to be observed.

Nitric oxide, NO, is naturally present in heated air flows such as the ones examined here. This situation is often preferable to seeding a chemical species into the flow which can often be impractical or it may influence the dynamics of the flow. NO has some advantageous spectroscopic properties that make it an excellent choice for PLIF thermometry. NO has excited-state radiative lifetimes that are independent of rotational quantum number and it also exhibits strong non-resonant fluorescence which alleviates problems associated with radiative trapping and laser scatter. The spectroscopy of NO is also very well characterised which significantly aids in data analysis and modelling. At present, only room temperature experimental data exists which shows the independence of excited state collisional quenching rates on rotational quantum number. The present work also assumes this independence for elevated temperatures since this simplifies the analysis immensely and no contrary evidence exists. Quenching rates can be included in the analysis if it eventually proves necessary, however this would be at the expense of the simplicity currently associated with the technique.

Applying PLIF to free-piston shock tunnels provides a unique set of experimental problems not encountered in other flow facilities. Real gas effects are prominent and the high temperature and pressure variations in the imaged region mean careful consideration of PLIF imaging parameters is necessary. Metallic contaminants which are eroded from the shock tube walls produce strong emission in high temperature regions in the flowfield. This background emission can easily swamp fluorescence signals, so careful spectral filtering is necessary (Palma et al. 1993). Conventional transmission filters were found to be unsuitable since they attenuate the signal by as much as 80%. By using a narrowband dielectric mirror however, narrowband filtering can be employed without significant loss of signal. The aim of the work presented here is to determine whether PLIF can be applied quantitatively to free-piston shock tunnels and

what are the important parameters which need to be considered.

THEORY

The theory of PLIF thermometry has been well described elsewhere and is not reviewed here (see Seitzman et al. 1994, Palmer et al. 1994). Essentially, PLIF gives a relative measure of the population of the probed state. If two different rotational states are probed and the ratio of the signals taken, the other signal dependencies (fluorescence yields, quenching rates, collection efficiencies etc.) cancel out and the ratio is only dependent on the temperature. Different transition pairs have different temperature sensitivities and careful choice of the pair of transitions is necessary. Collisional broadening and shifts of absorption lines are also a major concern in shock tunnel flows due to the large pressure and temperature variations. Since these effects are independent of rotational state they can be eliminated from the signal ratio. However, if the overlap between the laser spectral profile and the absorption line is significantly reduced, the fluorescence signal may become too weak to detect against background flow luminosity or camera noise.

For PLIF thermometry in unsteady or turbulent flows it is necessary to use two lasers and cameras to excite the two transitions in rapid sequence. However, for steady flows it suffices to use one laser and camera and assume a degree of shock tunnel repeatability by taking images on successive shots of the tunnel. The latter method has been employed here.

EXPERIMENT

The experiments were performed on the T2 free-piston shock tunnel (Stalker 1967) at the Australian National University. The T2 nozzle is a 30 degree full angle conical geometry with a 6.4 mm diameter throat and an area ratio of 144. The same flow conditions were used for both cylinder and wedge experiments. The primary shock speed was measured to be 1.90 km/s which gives a flow enthalpy of 4.1 MJ/kg. The nozzle reservoir pressure was 28.4 MPa and the calculated reservoir temperature was 3320 K. The freestream pressure and temperature were calculated to be 3 kPa and 340 K respectively and the freestream NO concentration was calculated to be 5%.

A schematic of the experimental set up is shown in Fig. 1. A cell containing high pressure hydrogen (1 MPa) is used to Raman-shift the output of a tunable excimer laser (Lambda Physik EMG150ETS) operating with KrF at 248 nm. The first anti-Stokes order is separated from the other orders with a Pellin-Broca prism and formed into a sheet using a 40 mm focal length cylindrical lens and a 1000 mm focal length spherical lens. The sheet was 80 mm wide and loosely focussed to approximately 1 mm thickness. This radiation is tunable between 224.9 and 225.4 nm which coincides with the $A^2\Sigma^+ \leftarrow X\ ^2\Pi$ (0,0) band of NO. A small portion of the beam is split off and used for wavelength calibration by passing it through a $H_2 + O_2$ flame. The laser-induced fluorescence (LIF) from the flame is imaged onto a 0.5 m spectrometer (which acts as a 9 nm bandpass filter), allowing LIF from only the NO (0,1) vibrational band near 236 nm to be detected. The energy of the Raman shifted beam was

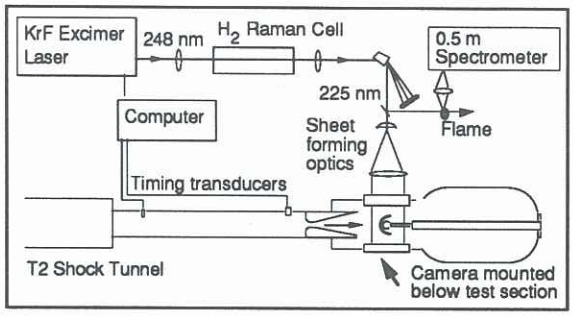

FIGURE 1: SCHEMATIC OF EXPERIMENTAL ARRANGEMENT.

typically 4 mJ per pulse with a linewidth of approximately 0.25 cm^{-1}.

The laser is tuned to a particular rotational line prior to each firing of the shock tunnel. Immediately before firing, the tunnel operator stops the laser via a remote switch. After firing, the nozzle reservoir pressure transducer detects the shock reflection at the end of the shock tube and the laser is fired 450 μs later, this delay being chosen so as to coincide with the period of steady flow. An intensified CCD camera (in house assembled dual MCP fibre optically coupled to an 8-bit CCD, 512 by 240 pixels, 250 ns gating period) is used to capture the fluorescence image at right angles to the laser sheet. The fluorescence is turned through 90 degrees by reflecting it off a dielectric mirror (normal incidence KrF excimer mirror) which has maximum reflectance between 210 and 240 nm. A 2 mm thick UG-5 Schott glass filter is used to block off elastic scatter at the laser wavelength, thus allowing only the (0,1) vibrational band at 236 nm through to the camera. The dielectric mirror and short camera gating time were able to efficiently filter out the broadband background contaminant emission.

The variation in energy across the laser sheet is measured simultaneously by use of a dye cell and CCD camera (Seitzman et al 1994). This energy distribution measurement is then used to correct the PLIF image and it also takes account of any pulse to pulse fluctuations in the total laser energy.

RESULTS AND DISCUSSION

Within the tuning range of the laser only a limited number of lines are suitable for thermometry. It is preferable to choose lines that are spectrally isolated to prevent PLIF contributions from nearby transitions (the absorption line profile broadens and shifts throughout the flowfield due to the pressure and temperature variations). Transitions with relatively low absorption coefficients are preferable to prevent both excessive beam attenuation across the imaged region and also to prevent saturation of the transition. The beam attenuation problem is also dependent on the NO concentration in the flow which in the current situation can not be altered without changing the flow conditions.

For both flowfields considered here, three transitions were chosen with a large variation in rotational quantum number J, while trying to satisfy the above criteria. The J=18.5 transition was the lowest J available within the tuning range while the J=38.5 was one of the highest, giving a $\Delta E/k \sim 3041$ K, where ΔE is the energy separation

between the rotational levels from which the transitions originate and k is the Boltzmann constant. When images from these transitions are combined, temperatures in the range 1000 K to 3200 K are measurable with current detection system. Since the freestream has a temperature of about 300 K a third line was chosen (J=27.5) which, when combined with the J=18.5 line, can be used to determine temperatures between 300 K and 1000 K.

In figure 2, images (a) to (c) show the corrected PLIF images for each of the three transitions chosen. Each image is the average of five single shot images, each of which was corrected for background luminosity and laser energy variation across the sheet. In each image the flow is entering from the left and the laser sheet from the top producing the shadow region beneath the model. In image 2(a) the signal is strong in the freestream and decreases across the shock as the population of the J=18.5 level varies. This image also allows the edges of the nozzle core flow to be easily observed. In images 2(b) and 2(c) the freestream signal decreases with increasing J since these rotational levels are less populated. Images 2(a) and 2(b) are divided together and the ratio is used to derive a temperature map as shown in 2(d). Image 2(d) shows the freestream temperature and everything behind the shock can be considered invalid since temperatures much higher than 1000 K (and those much lower than 300 K) require a fluorescence ratio between the images which exceeds the dynamic range of the 8-bit CCD camera. The temperature calculation assumes that the optical collection efficiencies for both images are equal, which is a very good assumption since exactly the same experimental arrangement is used for both images. A freestream temperature of 320 K was derived from this image by averaging over a small uniform region in the freestream to reduce random noise. Image 2(e) is used to determine the higher temperatures behind the shock. Temperatures of about 3200 K were expected in the stagnation region in front of the body but only 2000 K is measured from 2(e). The discrepancy is undoubtedly due to high collisional quenching rates in this region (pressure = 300 kPa) which, as can be seen from images 2(a) and 2(b), has significantly reduced the fluorescence signal intensity to below the limit of sensitivity of the camera. Away from the stagnation region the temperatures begin to approach the values predicted by preliminary CFD calculations.

For the case of the wedge, the same process as with the cylinder was followed. Figure 3 shows the wedge images for the three transitions used and the two derived temperature maps. In these images the oblique shock (49°) curves as it interacts with the expansion from the corner. The edge of the core flow occurs near the top of the image. The freestream temperature measured here was 300 K while behind the shock a maximum temperature of 1500 K was measured. The calculated temperature behind this oblique shock is about 1800 K. Image 3(a) shows signs of saturation in the freestream which would tend to lower the measured temperatures. Behind the shock this would not be as important since the pressure here would significantly increase the rotational transfer rate and hence reduce the chance of saturating the transition.

Apart from saturation of the $^{S}R_{21}(18.5)$ transition, there was also a noticeable amount of laser beam attenuation (approx. 20%) across the freestream due to absorption (see figure 2(a)).

Higher Enthalpy Shots

Several shots were performed at a 14~MJ/kg condition to ascertain the effectiveness of the filtering used to eliminate the background contaminate emission. The 35° half angle symmetric wedge was used since with the current filtering there was too much emission to go above 4 MJ/kg with the cylinder. The images obtained show only a small amount of flow luminosity which could be easily corrected for in a PLIF experiment. For bluff body work at higher enthalpies it would be necessary to improve the filtering, perhaps by using several reflection filters in series.

CONCLUSIONS

PLIF imaging of NO in a shock tunnel flow has been presented. A Raman-shifted tunable excimer laser has been used to probe naturally occurring NO in hypersonic flows over a cylinder and a wedge. The measured freestream temperatures show excellent agreement with theory and the discrepancy behind the shock for the cylinder case has been attributed to collisional quenching of the excited-state population. Shots performed at 14 MJ/kg on a wedge demonstrate the effectiveness of the filtering employed to remove background emission. Rotational and Vibrational PLIF temperature measurements are currently in progress at this higher enthalpy condition. Using a tunable dye laser to increase the laser tuning range, it should be possible to find suitable transitions to reduce the effect of beam attenuation due absorption and transition saturation.

ACKNOWLEDGMENTS

The authors would like to thank Paul Walsh for his technical assistance. This work was funded by the Australian Research Council.

REFERENCES

Houwing, A. F. P., Boyce, R. R., Palmer, J. L., Thurber, M. C. Wehe, S. D., Hanson, R. K., 1994, "Flow Imaging and Thermometry using Planer Laser Induced Fluorescence in a Shock Tunnel Flow", AIAA PAper No. 95-0515.

Palma, P. C., Houwing, A. F. P., Sandeman, R. J., 1993, "Absolute intensity measurements of impurity emissions in a shock tunnel and their consequences for laser induced fluorescence experiments", *Shock Waves*, Vol. 3, pp. 49-53.

Palmer, J. L., Houwing, A. F. P., Thurber, M. C., Wehe, S. D., Hanson, R. K., 1994, "PLIF imaging of transient shock phenomena in hypersonic flows", AIAA Paper No.94-2642

Seitzman, J. M., Hanson, R. K., DeBarber, P. A., Hess, C. F., 1994, "Application of quantitative two-line OH PLIF for temporally resolved planar thermometry in reacting flows", *Applied Optics,* Vol. 33, pp. 4000-4012.

Stalker, R. J., 1967, "A study of the free-piston shock tunnel", *AIAA Journal,* Vol. 5, pp. 2160-2165.

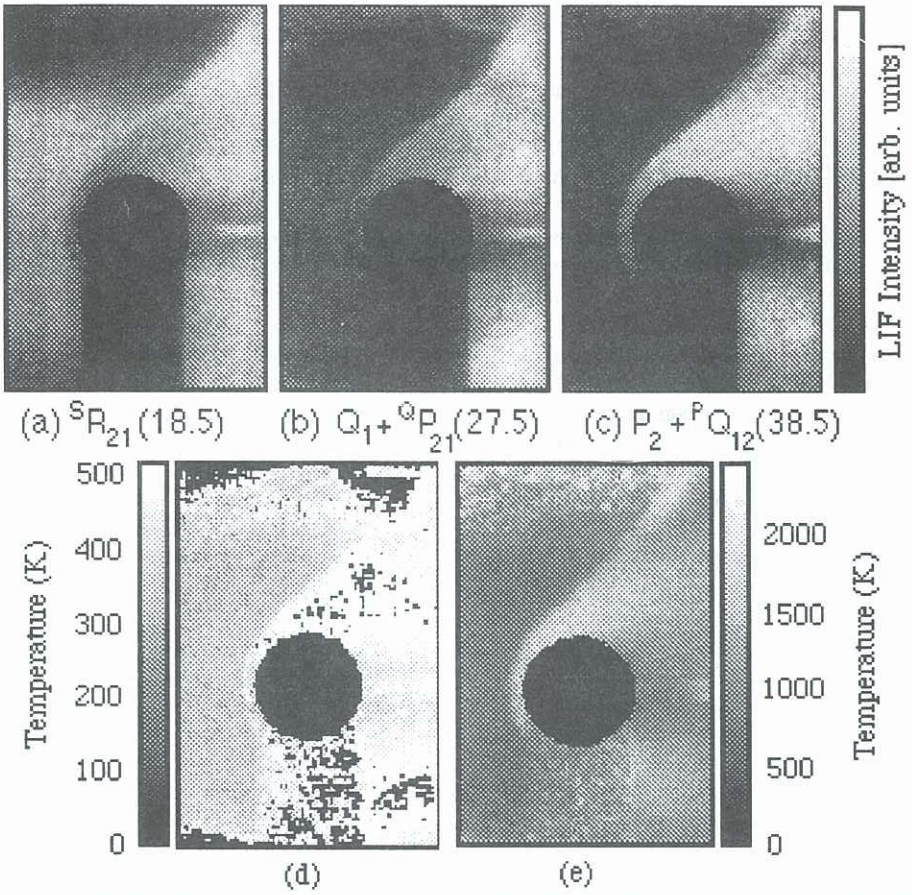

FIGURE 2: PLIF IMAGES OF THE MACH 7 FLOW OVER A CYLINDER. IN EACH IMAGE THE FLOW IS FROM LEFT TO RIGHT AND THE LASER ENTERS FROM THE TOP.

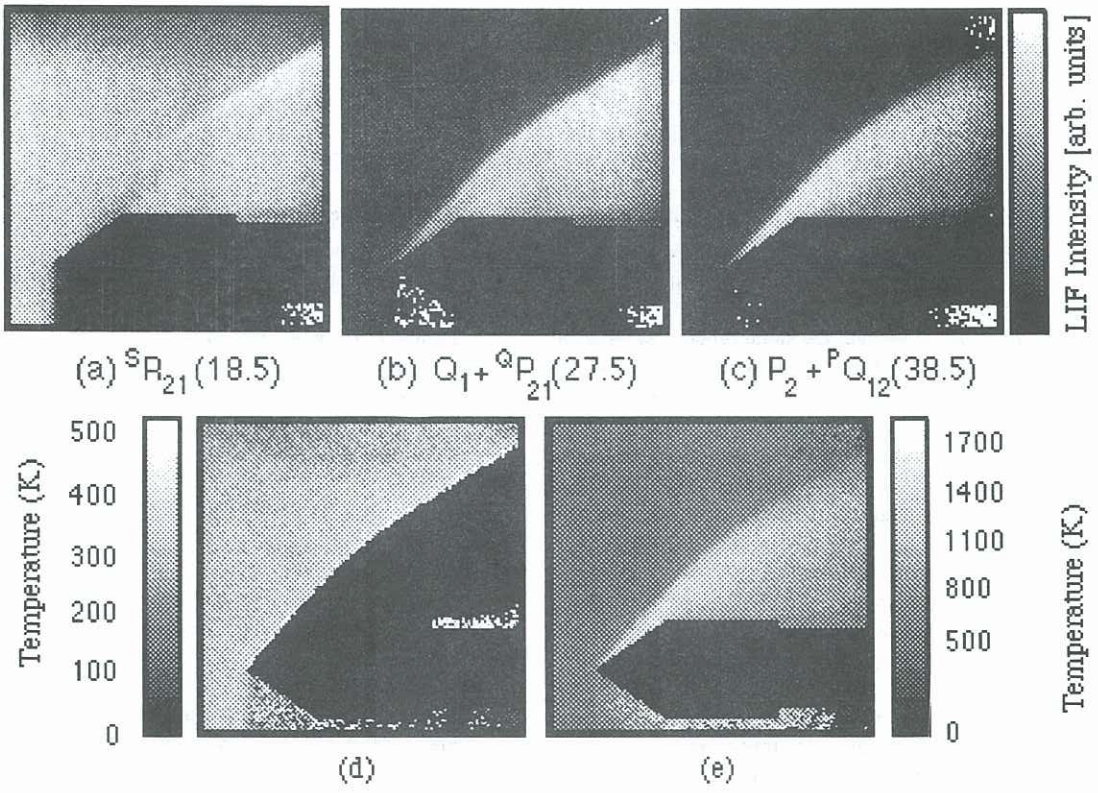

FIGURE 3: PLIF IMAGES OF THE MACH 7 FLOW OVER A 35° WEDGE. IN EACH IMAGE THE FLOW IS FROM LEFT TO RIGHT AND THE LASER ENTERS FROM THE TOP.